

Atomic and electronic structure of crystalline and amorphous alloys. I. Calcium-magnesium compounds

S. S. Jaswal* and J. Hafner

Institut für Theoretische Physik, Technische Universität Wien, Karlsplatz 13, A-1040 Wien, Austria

(Received 9 October 1987; revised manuscript received 13 April 1988)

Calculations of the atomic and electronic structure of Ca-Mg glasses and of the crystalline intermetallic compound CaMg_2 are presented. For the glasses, the calculations are based on realistic models of the atomic structure constructed by a molecular-dynamics computer simulation linked to a steepest-descent potential-energy mapping. Interatomic forces are described in terms of pseudopotential-derived effective pair potentials. Our results for the atomic structure are in very good agreement with x-ray-diffraction data. They show that the topological short-range order in the glass is similar to the atomic arrangement in the crystalline Laves phase and best described as a highly defective tetrahedral close packing. The analogy between the glassy and the crystalline phases extends to the electronic structure. In both the crystalline and the amorphous alloys we find an essentially free-electron-like density of states (DOS), but close to the Fermi level the DOS is enhanced due to the onset of Ca $3d$ states. We find no evidence for the existence of a structure-induced minimum in the DOS near E_F . Our results are in good agreement with photoemission measurements and electronic specific-heat data.

I. INTRODUCTION

The knowledge of the valence-band structure of a solid is significant for the understanding of its physical and chemical properties. In the crystalline state the adequate description is based on the Bloch theorem and consists of the dispersion relations $E_n(\mathbf{k})$ of the energy eigenstates and of the density of states $n(E)$. In the amorphous or liquid state the wave vector \mathbf{k} is no longer a good quantum number, but the concept of density of states is still meaningful. Nagel and Tauc¹ extended the stability criterion for certain intermetallic compounds known as Hume-Rothery phases to simple-metal glasses. The starting point is the explanation of Hume-Rothery critical valence-electron concentrations proposed by Mott and Jones.² They showed that at these critical concentrations the spherical Fermi surface of the quasifree valence electrons just touches a Brillouin-zone plane of the stable crystalline structure, i.e., we have $|\mathbf{Q}| = 2k_F$, where \mathbf{Q} is a vector of the reciprocal lattice. If this condition is satisfied, an energy gap of width $2w(\mathbf{Q})$ (w is the relevant pseudopotential matrix element) opens in the energy band. This gap induces a minimum in the density of states at $E = E_F$ and contributes to the lowering of the electronic ground-state energy.

In the amorphous phase there are no reciprocal-lattice vectors and hence no counterparts to the crystalline band gaps. The structural information is contained in the spherically symmetric static structure factor $S(Q)$, which has a well-defined first peak at $Q = Q_p$. The amplitude of this peak is a measure for the remaining structural correlations in the glassy state. Nagel and Tauc suggested that these correlations are strong enough to induce a minimum in the density of states. If, in analogy to the Mott-Jones condition, we have $Q_p = 2k_F$, this structure-

induced minimum in the density of states (DOS) would contribute to a lowering of the total energy of the amorphous phase relative to the competing crystalline phases.

The Nagel-Tauc model and its various implications have been widely discussed in the literature. The first attempts concentrated on the classical transition-metal-based metallic glasses. However, it turned out that in the case of the inter-transition-metal glasses (Fe-Zr, Co-Zr, etc.) the electronic structure is dominated by strong d - d interactions which are manifested in the DOS by a distinct splitting of the d bands depending on the relative position of the alloy constituents in the Periodic Table and on their concentrations.³ In the transition-metal-metalloid glasses the structure of the DOS is determined by a strong p - d hybridization.⁴ In both cases the DOS at the Fermi level is dominated by a high d component and no structural correlations could be established. The amorphous alloys of noble metals with polyvalent metals have been widely studied.^{5,6} The investigations of the electronic transport properties,⁵ the atomic structure, and the stability of these glasses⁶ confirm the existence of a strong structural correlation, and in Au-Sn and Cu-Sn alloys the existence of a DOS minimum at the Fermi level has indeed been confirmed by photoemission spectroscopy.^{7,8} Thus the glasses formed by noble metals and polyvalent metals can rightfully be considered amorphous Hume-Rothery phases,⁵ just as their crystalline counterparts.⁹ For the metallic glasses formed by simple metals only, the situation is less clear. Photoemission spectra of Ca-Al (Ref. 10) and Mg-Zn (Ref. 11) glasses have been interpreted as indicating a Nagel-Tauc minimum, but the evidence is really not so convincing. Specific-heat data for both Ca-Al and Ca-Mg (Ref. 12) alloys show that the DOS at the Fermi level is enhanced rather than reduced against the free-electron value.

What is most sorely missing is a self-consistent electronic-structure calculation based on a realistic model of a simple-metal glass to verify the Nagel-Tauc conjecture and to better understand the electron-transport properties, specific-heat data, and photoemission spectra. Preliminary results of such a study have been reported in a recent article.¹³ Here we extend the investigations to detailed calculations of the electronic structure of glassy and crystalline Ca-Mg alloys.

As we shall deal with simple, *s-p*-bonded alloys, we can base our approach on interatomic forces calculated in the linear-response and pseudopotential formalism.^{14–16} The next step is the modeling algorithm, which should be sufficiently sensitive to the details of the interatomic forces. We adopt a molecular-dynamics simulation of the liquid phase linked to a steepest-descent mapping of the instantaneous configurations of the liquid onto local potential-energy minima.^{17–19} The removal of the thermally induced distortions through the mapping results in a significant image enhancement of the local order. It has been proposed^{17,20–22} (and we verify by a detailed comparison with diffraction data) that this “inherent structure” of the liquid is a very good model of the amorphous state. This then serves as basis of the electronic-structure calculations.

The perturbation methods used for the calculation of the interatomic forces cannot be used for the calculation of the electronic DOS. In fact, it has been shown long ago that although low-order perturbation theory yields well-converged results for any quantity related to the integrated DOS (like the total energy or the interatomic forces), it is inappropriate for the calculation of all quantities related to the differential DOS (see, e.g., Ref. 15, p. 336). The choice of a method for the calculation of the DOS must be guided by the following criteria: (a) The calculation should be self-consistent (self-consistency was the major breakthrough in the electronic-structure calculations for the crystalline state). (b) Our atomic-structure calculations reveal substantial fluctuations in the coordination numbers, bond distances, etc. Therefore, the self-consistency should be achieved at the individual rather than the average atomic level. Because of the enormous computational effort required for such a study, we simulate the glass with a supercell with periodic boundary conditions and use the highly efficient linearized-muffin-tin-orbital (LMTO) method for the electronic-structure calculations.

Ca-Mg has been chosen as starting point of our study, because it is (except for perhaps Mg-Zn) the simplest metallic glass whose atomic and electronic structure have been investigated experimentally. The atomic structure of glassy Ca-Mg is found to be of a tetrahedrally close-packed type with many sites of icosahedral symmetry, in rather striking analogy to the stable crystalline phase CaMg₂. The difference between the crystalline and glassy phases is essentially in the larger number of topological defects in the amorphous phase. The electronic structures of both the crystalline and amorphous phases are examined in detail. The DOS starts out essentially as free-electron-like, but is enhanced over the free-electron value near the Fermi level due to the onset of the Ca *d*

states. A detailed investigation shows that the *s-p* hybridization seems to be slightly reduced compared to pure Mg, but reveals no trace of a structure-induced minimum.

Thus, unlike the noble-metal-based glasses, the formation of glassy Ca-Mg is not related to a Nagel-Tauc (or Hume-Rothery) criterion. This is not surprising, because the formation of the crystalline phase is dominated by geometrical packing effects. We find that they dominate the properties of the glassy phase as well.

II. STRUCTURE MODELING

The calculations of the interatomic potentials has been described in detail in the previous work on liquid,²³ crystalline,²⁴ and glassy^{23,25} Ca-Mg alloys. Due to the chemical similarity of both components, the interatomic potentials change only slightly upon alloying. The work on the glassy phases was based on a static relaxation of a dense-random-packing starting structure by energy minimization. In this case the local order in the glassy phase is determined to a large degree by the choice of the initial configuration. The “potential-energy-mapping” technique is entirely independent of the choice of a starting structure and very sensitive to the details of the interatomic interactions.

The simulation sets out with a molecular-dynamics calculation for the liquid alloy—this ensures that after an equilibration phase the local order (both chemical and topological) is really that corresponding to the interatomic forces and to the thermodynamic variables. Parallel to the calculation of the phase-space trajectory, independent instantaneous configurations are periodically mapped onto local minima of the potential energy. This is achieved by setting the velocities of all particles to zero (thus removing the kinetic energy) and by following a steepest-gradient path on the potential-energy hypersurface from the instantaneous configuration to a nearby potential-energy minimum. In this way the configuration space is divided into classes of configurations, each configuration within a given class being associated with the same local potential-energy minimum. It is not surprising that the quench pair-correlation functions $g_{ij}(R)$ obtained by taking an average over the configurations corresponding to a local minimum in the potential energy show a substantial image enhancement over the equilibrium pair-correlation functions of the liquid phase. It was surprising, however, when Stillinger and Weber¹⁷ showed that the quenched correlation functions are entirely independent of the thermodynamic state of the system before the quench. The simulations of Stillinger and Weber refer to isochoric conditions, i.e., the atomic volume of the quenched state is the same as that of the liquid. Of course, this is not a physically realistic situation. In our study we have been able to show that the same result also holds if we allow for a variation of the atomic volume. We also find that it holds independently of the “quench path” adopted: We can either (a) “quench” at the constant volume of the liquid and compress the quenched state at $T=0$ K until the zero-pressure equilibrium condition is met, or (b) compress the

liquid at constant temperature to the density of the "glass" and quench afterwards at constant volume, or (c) compress (by scaling of the coordinates) simultaneously with the removal of the kinetic energy. In either case (a), (b), or (c) the resulting correlation functions for the quenched state agree within the statistical fluctuations.

This important result has two consequences: (a) It shows that the liquid has a temperature-independent inherent structure, and any variation of the pair correlations results from thermally induced distortions of the locally stable configurations. (b) The potential-energy mapping constitutes a very attractive algorithm for modeling the structure of the amorphous phase.^{18,19} The resulting structure is entirely independent of the thermodynamic parameters before the quench and determined solely by the interatomic forces. In fact, the mapping corresponds to an infinitely rapid quench without subsequent structural relaxations (any crossing of potential-energy saddle points is carefully avoided by the steepest-descent procedure).

Our calculation for the Ca-Mg system is based on a sample of 800 atoms enclosed in a rhombic dodecahedron with periodic boundary conditions. The constant-energy molecular-dynamics calculations have been performed with the simple Verlet algorithm²⁷ with a time step of $\Delta t = 10^{-15}$ s. About 2000 time steps were used for equilibration and 3000 for calculating ensemble averages. Several runs at temperatures ranging between $T \sim 873$ and 2073 K were performed (temperatures are calculated from configuration averages over the kinetic energy).

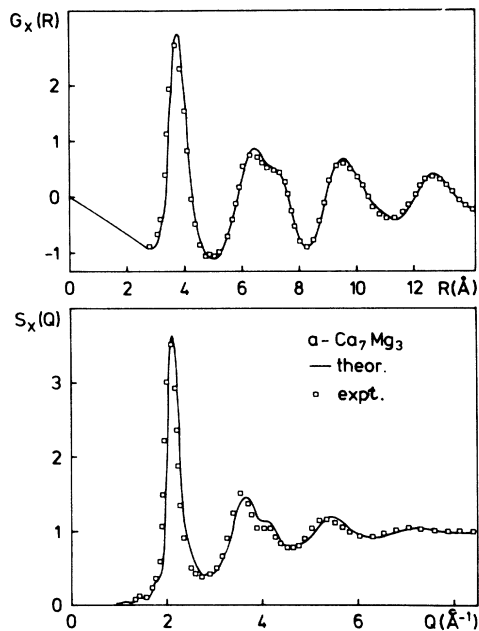


FIG. 1. Composite (x-ray- and Debye-Waller-factor-weighted) static structure factor $S_x(Q)$ and reduced pair distribution function $G_x(R)$ for amorphous Ca_7Mg_3 . The solid line represents the result of the computer simulation (averaged over 20 independent configurations) and the open circles show the x-ray-diffraction data of Nassif *et al.* (Ref. 28).

The steepest-descent algorithm is described in previous publications.²⁰⁻²² Every 150 time steps the instantaneous configuration of the liquid was mapped onto a nearby potential-energy minimum, and correlation functions of the quenched phase are based on averages over 20 projected configurations. A very detailed description of the molecular-dynamics plus potential-energy-mapping procedures is given in Ref. 22.

For Ca-Mg glasses, only an x-ray-diffraction experiment²⁸ measuring a weighted structure factor is available. The computed equilibrium density of the quenched state ($n = 0.0275 \text{ \AA}^{-3}$) agrees well with the experimental number density of the glass ($n = 0.0269 \text{ \AA}^{-3}$). In Fig. 1 we compare the composite static structure factor $S_x(Q)$ (the partial structure factors resulting from the potential-energy mapping are weighted with the x-ray-scattering form factors and partial Debye-Waller factors) and the reduced pair distribution function $G_x(R)$ [obtained by Fourier-transforming $S_x(Q)$] with the experimental data. The agreement is found to be very good.

More information is contained in the partial correlation functions. These are shown in Figs. 2 and 3 for quenched CaMg_2 and Ca_7Mg_3 alloys. Stillinger and La Violette²⁹ have pointed out that the best single indicator

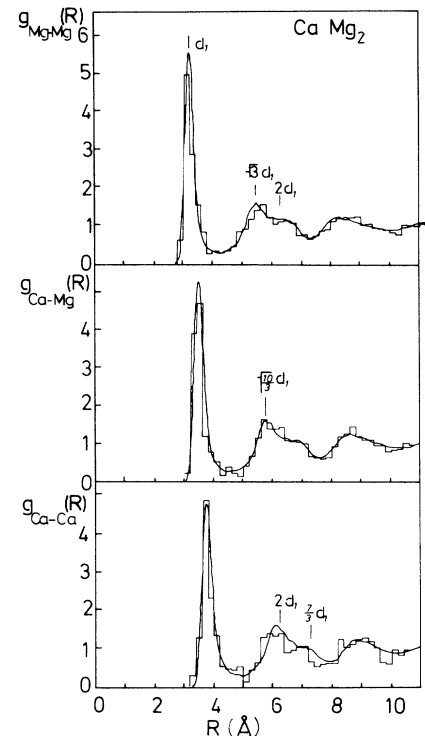


FIG. 2. Partial pair-correlation functions $g_{ij}(R)$ for a quench-condensed CaMg_2 alloy. The solid lines show the computer-simulation result obtained by the potential-energy mapping of 20 independent configurations. The histogram represents the correlation functions of a single 60 atom model prepared out of one of these configurations (see text). The vertical bars indicate the interatomic distances in the Laves phase (d_1 is the shortest Mg-Mg distance).

for the form of the quenched correlation functions is the stable crystal structure of the given substance. For CaMg_2 this is the hexagonal MgZn_2 -type Laves phase. Indeed, we find that the first and second peaks of the pair-correlation functions of the quench-condensed CaMg_2 alloy may be indexed in terms of the interatomic distances in the Laves phase. The coordination number of the Ca atoms in the crystal is 16 and that of the Mg atoms is 12. The Mg sites are centers of regular icosahedra, and the Ca sites those of Friauf polyhedra that may be considered as being derived from the icosahedron by the introduction of topological defects.³⁰ In the quench-condensed phase the coordination numbers of the Mg atoms are distributed around 12 and those of the Ca atoms around 15, but with substantial fluctuations. The average coordination number ($N_c = 12.94$ for CaMg_2 , $N_c = 13.30$ for Ca_7Mg_3) is very close to that of the Laves phase ($N_c = 13.33$) (see Fig. 4). For the quench-condensed Ca_7Mg_3 phase we find again that the interatomic distances between the Ca atoms are very similar to those in a Laves phase, but the Mg-Mg and Ca-Mg distances show appreciable deviations (Fig. 3).

Thus, both quench-condensed alloys represent defective tetrahedrally close-packed structures. The essential difference between the structures obtained by quenching the compound-forming alloy (CaMg_2) and the glass-forming alloy (Ca_7Mg_3) consists of the much higher number of topological defects in the latter. (It might appear premature to draw this conclusion on the evidence presented here. In Ref. 22 we have presented a more complete analysis of a series of glass-forming and

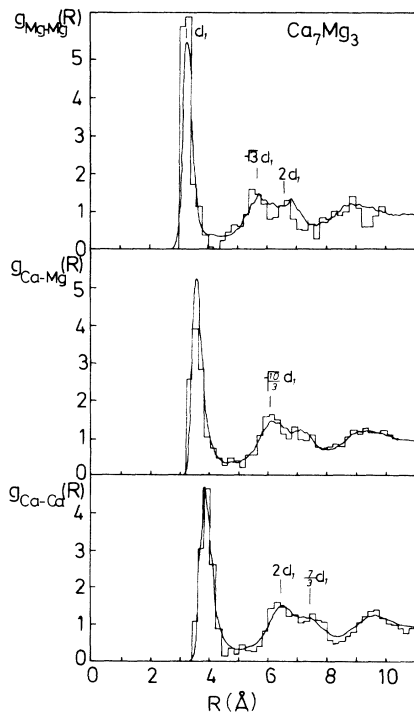


FIG. 3. Partial pair-correlation functions $g_{ij}(R)$ for a quench-condensed Ca_7Mg_3 alloy. See Fig. 2.

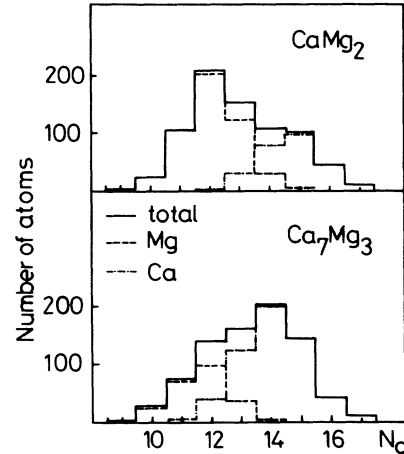


FIG. 4. Distribution of the nearest-neighbor coordination number in amorphous CaMg_2 and Ca_7Mg_3 .

compound-forming alloys with a more detailed description of the potential-energy-mapping algorithm.) The 800-atom configuration we used for a meaningful comparison with the diffraction data is too large to serve as a basis for the supercell method for the calculation of the electronic DOS to be presented below. We prepare smaller models containing about 60 atoms by cutting small cubes of appropriate size out of the 800-atom cells. The origin of these cubes is chosen such that the cube contains atoms of both species in the proper ratio and that, if the cube is periodically repeated, there are only minimal strains across its surfaces. The remaining strains are relaxed by a static energy minimization.

Figures 2 and 3 show, besides the correlation functions calculated by averaging over twenty 800-atom configurations, the correlation functions calculated from a typical 60-atom model. Of course, the statistical fluctuations are now much more pronounced, but the characteristic pattern including the correlation with the local geometry of the Laves phase is surprisingly well preserved. To ensure a good statistical representation of the glass, the DOS has been calculated from several different models taken from independent configurations.

III. THE ELECTRONIC STRUCTURE OF AMORPHOUS AND CRYSTALLINE Ca-Mg ALLOYS

The methods used for the calculation of the electronic structure of amorphous materials fall into three distinct classes: (a) effective-medium approaches, (b) computer simulations, and (c) cluster or supercell calculations. Effective-medium calculations³¹ retain only averaged structural information, are far from reaching electronic self-consistency, and yet are computationally very expensive. Computer simulations (equation-of-motion³² and recursion calculations^{33,34}) allow one to include the full structural information. However, until now it has been possible to achieve electronic self-consistency only for an average atom,³⁴ and not for each atom individually. In view of the rather important fluctuations in the local

geometry (see Fig. 4), this appears to be a serious limitation. The cluster³⁵ and supercell methods seem the most suitable to achieve local self-consistency. Scattered-wave calculations on finite clusters³⁵ are seriously limited by the influence of the free surface. Thus, for the time being the supercell method³⁶ seems to be the optimal choice, provided that the periodically repeated cell that can be handled with the available computer facilities is large enough. Our analysis of the 60-atom correlation functions suggests that this is the case.

For the supercell calculations we have the entire range of modern band-structure methods at our disposal. In principle, we could use the pseudopotentials from which the interatomic potentials have been derived. However, we must remember that a pseudopotential is not unique; we have the freedom to impose various criteria to give the pseudopotential various desirable properties.¹⁴⁻¹⁶ As the calculation of the interatomic forces is based on low-order perturbation theory, it is essential to use a pseudopotential for which an optimal convergence of the perturbation series is achieved.³⁷ In exchange, these pseudopotentials have Fourier components with very large momentum transfers, making it difficult to use them in a band-structure calculation, especially for cells that are as large as those we intend to use. One possibility would be to switch to the "norm-conserving" pseudopotentials³⁸ better suited to this purpose (but not for the perturbation calculation of the interatomic forces). As we have to adopt another method anyway, we choose the linearized-muffin-tin-orbital (LMTO) method of Andersen^{39,40} because of its computational efficiency and because of personal expertise.^{36,41} The LMTO method has the additional advantage that using the "fast scaling" procedure self-consistency can be achieved with tolerable computational effort.

Usually, supercell calculations are done for the Γ point [as usual, this means, in fact, a very small wave vector, $\mathbf{k}=(0.0, 0.0, 0.01)(\pi/a)$] of the Brillouin zone only, a continuous DOS is derived from the discrete spectrum of

the Γ point eigenvalues by an appropriate Gaussian broadening (we use Gaussian with a width of 0.2 eV). For the relatively narrow bands of the transition-metal and rare-earth glasses, this is certainly an acceptable approximation.³⁶ For Ca_7Mg_3 we find that a calculation based on the Γ point only produces a DOS with appreciable structure (see Fig. 5), particularly just above the Fermi level. If we extend the calculation to four points in the Brillouin zone (taking the corners of the irreducible wedge), most of this structure disappears (Fig. 5). It is especially the calculation of DOS that is sensitive to the Brillouin-zone averaging; the self-consistent potential of the individual atoms is essentially the same for a Γ -point only or a four-point calculation. The necessity of including more than just the Γ point in the calculation of the DOS simply reflects the fact that the s, p bands of simple metals are not completely flat for the 60-atom cluster. This implies that one should consider a larger cluster to simulate a glass. Now, the step from a 60- to a 100-atom cluster will increase the cube edge of the cluster only by about 70% of the nearest-neighbor distance and therefore is not expected to give any new information. With our computer facilities it is not possible to consider bigger clusters. Fortunately, we are able to simulate a Γ -point calculation for a cluster with twice the cube edge of the smaller cluster (hence 8 times the number of atoms in the smaller cluster) by considering the electronic structure at the Γ , X , M , and R points in the Brillouin zone. This procedure neglects the disorder beyond the 60-atom cluster, but we expect this effect to be small.

In order to verify this point, we have recently used the average self-consistent potentials from the 60-atom supercell calculation to perform a tight-binding LMTO recursion calculation for the large 800-atom cluster from which the 60-atom model has been derived.⁴² The total and the partial DOS's from both calculations are in very good agreement. This shows that the procedure adopted here is indeed legitimate. The central-processing-unit (CPU) time for a self-consistent four-point calculation on

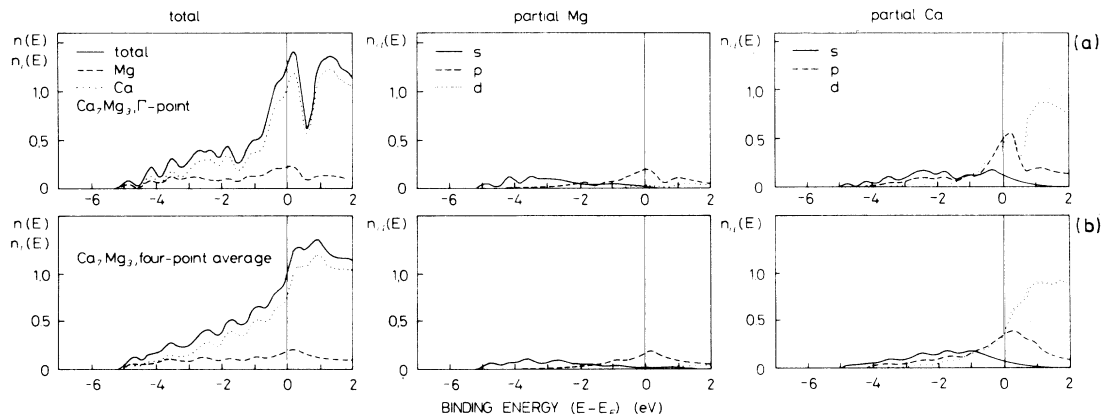


FIG. 5. Total, site-, and angular-momentum-decomposed electronic density of states (in states/eV atom) of amorphous Ca_7Mg_3 calculated for 60-atom cell using (a) the Γ -point energy eigenvalues and (b) an average over four symmetry points (see text).

a 60-atom supercell is about 7 h on a NAS-9600 computer— it is about the same for the non-self-consistent recursion calculation on the 800-atom cluster.⁴²

On the average, the charge transfer in the Ca and Mg atomic spheres is very small (in Ca_7Mg_3 an average Mg atom loses 0.14 electrons, a mean Ca atom gains 0.06 electrons), as expected for this homovalent alloy. The local charge fluctuations are much more important: The charge transfer ranges from +0.21 to -0.12 electrons for the individual Ca atoms and from -0.23 to -0.03 electrons for the Mg sites. Thus the local structural fluctuations are reflected in the electron density, and this emphasizes the need for a calculation that is self-consistent on a local level.

A. The electronic DOS of crystalline and amorphous CaMg_2

In Fig. 6 we show the total, site- and angular-momentum-decomposed density of states of the hexagonal Laves-phase CaMg_2 and of a hypothetical amorphous phase of the same composition. The DOS of the crystalline phase is strongly structured by the van Hove singularities, reflecting the geometrical properties of the MgZn_2 -type (structure report symbol $C14$) crystal structure with 12 atoms in the primitive cell. However, the general form of the DOS, and especially of the width of the occupied part of the conduction band, conform with a free-electron picture (the bandwidth is $W=5.9$ eV, and the free-electron value would be $W=6.2$ eV).

The DOS calculated for the “quenched” 60-atom model (four-point Brillouin-zone average and configuration average) is close to the free-electron parabola at higher binding energies and slightly enhanced over the free-electron value close to the Fermi energy. This enhancement is clearly due to the onset of the Ca $3d$ states. [According to our LMTO calculation, we have, on the average, 0.74 Ca $3d$ electrons. The free-electron

DOS at the Fermi level due to the remaining 1.75 s - p electrons/atom is $n_{s,p}^{\text{NFE}}(E_F)=0.46$ state/eV atom (NFE denotes nearly free electron), which is in very good agreement with the corresponding result $n_{s,p}(E_F)=0.44$ states/eV atom from the LMTO calculation.] Thus, even in the s,p component of the DOS there is no indication of a structurally induced minimum in the DOS at the Fermi level, although the Nagel-Tauc criterion $Q_p=2k_F$ is reasonably well satisfied: we have $Q_p=2.40 \text{ \AA}^{-1}$ from the number-density structure factor $S_{NN}(Q)$, and $2k_F=2.55 \text{ \AA}^{-1}$ (counting all electrons) and $2k_F=2.45 \text{ \AA}^{-1}$ (counting only the s and p electrons). The individual s and p densities of states at the Mg sites are quite similar to those in pure Mg (see Steiner *et al.*⁴³ for photoemission data of pure Mg and their analysis in terms of band-structure calculations) and characterized by a large degree of s,p hybridization. The total width of the occupied conduction band ($W=6.2$ eV) is slightly larger than in the Laves phase and just equal to the weighted averaged of the bandwidth of Mg ($W=7.3$ eV) and Ca ($W=4.3$ eV).

B. The electronic DOS of amorphous Ca_7Mg_3

The electronic density of states of the metallic glass Ca_7Mg_3 shows only a slightly different pattern: At higher binding energy the DOS remains distinctly below the free-electron parabola; at the Fermi level the DOS is now strongly enhanced over the free-electron value. The width of the band again corresponds to the concentration average over the pure metal bands. We find $n(E_F)=0.98$ states/eV atom, to be compared with the free-electron value of $n^{\text{NFE}}(E_F)=0.58$ states/eV atom. The calculated value is in good agreement with that inferred from the specific-heat data [$n(E_F)=1.01$ states/eV atom]. The same analysis as for amorphous CaMg_2 yields $n_d(E_F)=0.4$ states/eV atom (we count 0.54 Ca $3d$ electrons); the free-electron DOS of the remaining s - p elec-

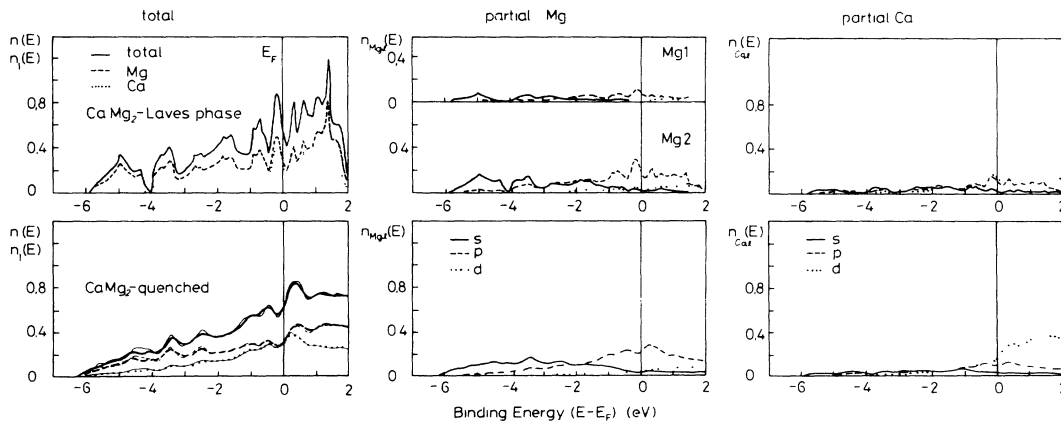


FIG. 6. Total, site-, and angular-momentum-decomposed electronic density of states (in states/eV atom) of crystalline CaMg_2 (MgZn_2 -type Laves phase) and of an amorphous CaMg_2 phase. The results for the amorphous phase have been calculated using four Brillouin-zone points and an average over two different configurations. The thin lines indicate the result obtained for a single configuration.

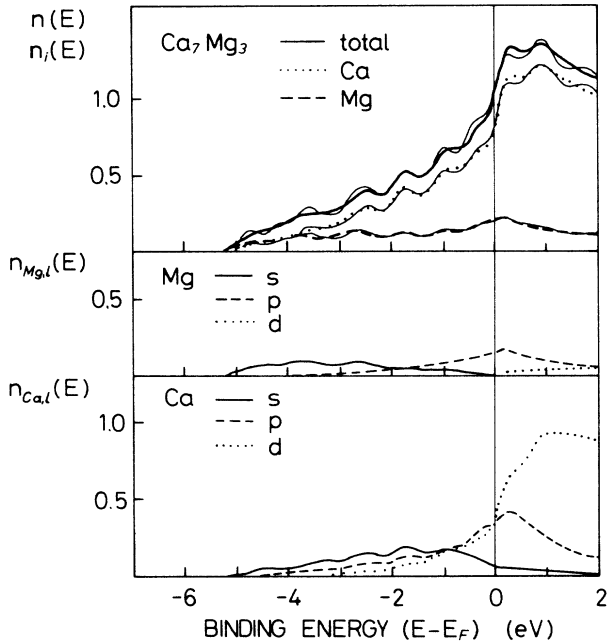


FIG. 7. Total, site-, and angular-momentum-decomposed electronic density of states (in states/eV atom) for amorphous Ca_7Mg_3 . See Fig. 6.

trons is $n_{s,p}^{\text{NFE}}(E_F) = 0.54$ states/eV atom, giving the total $n(E_F) = 0.94$ states/eV atom. Thus the enhanced DOS stems from the onset of the Ca d band, and again there is no indication for a structurally induced minimum in the DOS at the Fermi level, although the Nagel-Tauc criterion is satisfied [we have $Q_P \sim 2.20 \text{ \AA}^{-1}$ (taken from the

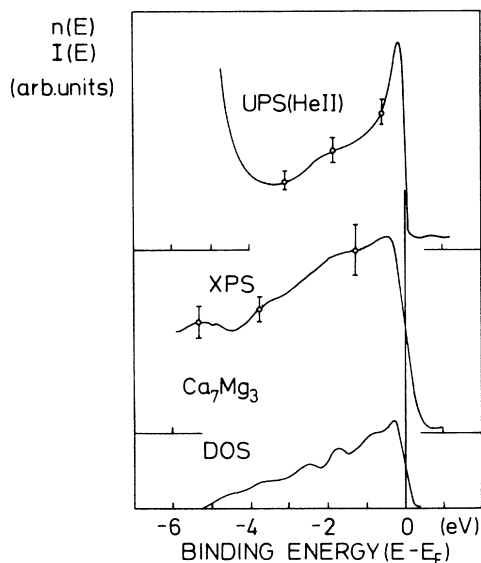


FIG. 8. Comparison of the calculated density of states of the Ca_7Mg_3 glass with XPS and UPS data (the unpublished results have been communicated by U. Mizutani and P. Oelhafen).

number-density structure factor $S_{NN}(Q)$, $2k_F = 2.34 \text{ \AA}^{-1}$ (counting all electrons) and $2k_F = 2.18 \text{ \AA}^{-1}$ (counting the s, p electrons only)].

The form of the DOS at higher binding energies is characterized by a reduced s, p hybridization of the Mg states, which is clearly a consequence of the reduced Mg-Mg overlap. The form of the DOS is well confirmed by recent photoemission data⁴⁴ of Mizutani and Oelhafen (Figs. 7 and 8). The general form of the x-ray-photoemission-spectroscopy (XPS) spectrum and the small structures at -2 and -4 eV correlate very well with the LMTO calculation. The ultraviolet photoemission spectroscopy (UPS) spectra are much more difficult to analyze due to matrix-element effects. In the present case the spectra are also affected by oxygen contamination (the strong onset near -5 eV in the UPS spectrum is due to this contamination).

IV. CONCLUSIONS

We have presented the first *ab initio* calculation of the atomic and electronic structure of a metallic glass. Our results for the Ca-Mg glasses show that the electronic density of states is essentially free-electron-like at higher binding energies, but has a substantial Ca d -electron contribution at the Fermi level. Near E_F the DOS is strongly increasing, and there is no indication of the structure-induced minimum at E_F postulated by Nagel and Tauc. The value of the DOS at E_F is in very good agreement with the measured electronic specific heat, and the form of the DOS is well confirmed by XPS data. The total bandwidth and DOS at the Fermi level are quite similar in the crystalline Laves-phase CaMg_2 and in the hypothetical amorphous-phase CaMg_2 . The differences between the electronic structures in the hypothetical glass CaMg_2 and the real glass Ca_7Mg_3 are small; they are just those expected from the change in composition. Thus, we find that there are similarities not only in the local order but also in the DOS in the Laves phase and in the metallic glass. We think that, like the Laves phase, the glass is properly interpreted as a size compound. The difference between the glass and the crystal is in the much higher number of topological defects in the glass, but its short-range order is still determined by the geometry of tetrahedral close packing.

Thus, the analysis of the electronic structure confirms our interpretation of Ca-based glasses given on the basis of pair-potential arguments alone.^{23,25} Energetically favorable packing is achieved by putting the nearest-neighbors into the first attractive minimum of the pair potential. That the packing is compatible with the form of the potential even for the more distant neighbors certainly contributes to the stability, but this effect is not strong enough to modify the electronic DOS, and nor are the electronic effects strong enough to induce a change in the structure dominated by size effects.

A closer inspection of the partial DOS points to a slight reduction of the s, p hybridization in amorphous Ca_7Mg_3 . Results on Ca-Al glasses [Ref. 13 and the following paper (paper II)] show that the incipient dehybridization of s and p states is much stronger in Ca-Al than in

Ca-Mg alloys. This and not a different degree of d character at the Fermi level might be responsible for the widely different properties of these metallic glasses.

Finally, we should perhaps point out that while the electronic-structure calculations are self-consistent, our approach does not achieve self-consistency between the atomic and electronic structure. Very recently, a method (the so-called density-functional molecular-dynamics method^{45,46}) has been proposed which aims at overcoming this deficiency. The density-functional molecular-dynamics technique must undoubtedly be considered a major breakthrough in condensed-matter simulations, but perhaps the results presented here are useful to eluci-

date some of the computational problems that must be solved before this method can be applied to simulations of metallic alloys (the electronic part of the method is based on supercell calculations quite similar to those described here).

ACKNOWLEDGMENTS

We are very grateful to Professor Uichiro Mizutani and Dr. Peter Oelhafen for communicating the results of their photoemission studies prior to publication. One of us (S.S.J.) acknowledges support from the Fulbright Foundation.

*On leave of absence from Behlen Laboratory of Physics, University of Nebraska, Lincoln, Nebraska 68588.

¹S. R. Nagel and J. Tauc, *Phys. Rev. Lett.* **35**, 380 (1975).

²N. F. Mott and H. Jones, *The Theory of the Properties of Metals and Alloys* (Oxford University Press, Oxford, 1936).

³P. Oelhafen, in *Glassy Metals II*, edited by H. Beck and H. J. Güntherodt, Vol. 53 of *Topics in Applied Physics* (Springer, Berlin, 1983), p. 283.

⁴T. Fujiwara, in *Amorphous Materials: Modeling of Structure and Properties*, edited by V. Vitek (AIME, Warrendale, PA, 1983), p. 221.

⁵U. Mizutani, *Prog. Mater. Sci.* **28**, 97 (1983).

⁶P. Häussler, in *Proceedings of the 3rd International Conference on the Structure of Non-Crystalline Materials*, edited by C. Janot and A. F. Wright [*J. Phys. (Paris) Colloq.* **46**, C8-361 (1985)].

⁷P. Häussler, F. Baumann, J. Krieg, G. Indlekofer, P. Oelhafen, and H. J. Güntherodt, *Phys. Rev. Lett.* **51**, 714 (1983).

⁸P. Häussler, F. Baumann, U. Gubler, P. Oelhafen, and H. J. Güntherodt, in *Proceedings of the Vth International Conference on Rapidly Quenched Metals*, edited by S. Steeb and H. Warlimont (Elsevier, Amsterdam, 1985), p. 1007.

⁹U. Mizutani and T. B. Massalski, *Prog. Mater. Sci.* **22**, 152 (1978).

¹⁰S. R. Nagel, U. Gubler, C. F. Hague, J. Krieg, R. Lapka, P. Oelhafen, H. J. Güntherodt, J. Evers, A. Weiss, V. L. Moruzzi, and A. R. Williams, *Phys. Rev. Lett.* **49**, 575 (1982).

¹¹P. Oelhafen, J. Krieg, and H. J. Güntherodt (unpublished).

¹²U. Mizutani, M. Sasaura, Y. Yamada, and T. Matsuda, *J. Phys. F* **17**, 667 (1987).

¹³J. Hafner and S. S. Jaswal, *J. Phys. F* **18**, L1 (1988).

¹⁴W. A. Harrison, *Pseudopotentials in the Theory of Metals* (Benjamin, New York, 1966).

¹⁵V. Heine and D. Weaire, in *Solid State Physics*, edited by H. Ehrenreich, F. Seitz, and D. Turnbull (Academic, New York, 1971), Vol. 24, p. 247.

¹⁶J. Hafner, *From Hamiltonians to Phase Diagrams—The Electronic and Statistical-Mechanical Theory of sp Bonded Metals and Alloys*, Vol. 70 of *Springer Series in Solid State Sciences*, edited by P. Fulde, M. Cardona, H. Queisser and K. von Klitzing (Springer, Berlin, 1987).

¹⁷F. H. Stillinger and T. A. Weber, *J. Chem. Phys.* **80**, 4434 (1984).

¹⁸T. A. Weber and F. H. Stillinger, *Phys. Rev. B* **31**, 1954 (1985).

¹⁹F. H. Stillinger and T. A. Weber, *Phys. Rev. B* **31**, 5262

(1985).

²⁰J. Hafner and A. Pasturel, *J. Phys. (Paris) Colloq.* **46**, C8-365 (1985).

²¹J. Hafner, in *Proceedings of the VIth International Conference on Liquid and Amorphous Metals*, edited by E. Lüscher and F. Hensel [*Z. Phys. Chem.* **157**, 115 (1988)].

²²J. Hafner, *J. Phys. F* **18**, 133 (1988).

²³J. Hafner, *Phys. Rev. B* **21**, 406 (1980).

²⁴J. Hafner, *J. Phys. F* **15**, 1879 (1985).

²⁵J. Hafner, *Phys. Rev. B* **28**, 1734 (1983).

²⁶J. Hafner, *Phys. Rev. B* **27**, 678 (1983).

²⁷L. Verlet, *Phys. Rev.* **159**, 98 (1967); see also D. W. Heermann, *Computer Simulation Methods in Theoretical Physics* (Springer, Berlin, 1986), p. 30.

²⁸E. Nassif, P. Lamparter, and S. Steev, *Z. Naturforsch.* **38a**, 1206 (1983).

²⁹F. H. Stillinger and R. A. La Violette, *J. Phys. Chem.* **83**, 6413 (1985).

³⁰D. R. Nelson, S. Sachdev, in *Amorphous Metals and Semiconductors*, edited by P. Haasen and R. I. Jaffee, *Acta-Scripta Metallurgica Proc. Ser. No. 3* (Pergamon, Oxford, 1986), p. 28.

³¹D. Nicholson, A. Chowdhary and L. Schwartz, in *Proceedings of the Vth International Conference on Liquid and Amorphous Metals*, edited by C. N. J. Wagner and W. L. Johnson [*J. Non-Cryst. Solids* **61&62**, 1137 (1984)].

³²J. J. Rehr and R. Alben, *Phys. Rev. B* **16**, 2400 (1977).

³³M. J. Kelly and D. W. Bullett, *J. Phys. C* **22**, 2531 (1979).

³⁴T. Fujiwara, in *Topological Disorder in Condensed Matter*, Vol. 46 of *Springer Series in Solid State Sciences*, edited by F. Yonezawa and Ninomiya (Springer, Berlin, 1983).

³⁵R. H. Fairlie, W. M. Temmermann, and B. L. Györfy, *J. Phys. F* **12**, 661 (1982); B. Delley, D. E. Ellis, and A. J. Freeman, *J. Phys. (Paris) Colloq.* **40**, C8-437 (1980).

³⁶S. S. Jaswal and W. Y. Ching, *Phys. Rev. B* **26**, 1064 (1982); W. Y. Ching, L. W. Song, and S. S. Jaswal, *ibid.* **30**, 544 (1984); S. S. Jaswal, *J. Non-Cryst. Solids* **75**, 373 (1985).

³⁷The criterion of Cohen and Heine (Ref. 14, p. 261) asks for the smoothest possible pseudo-orbital and ensures at the same time the maximum cancellation between the strongly attractive crystal potential and the repulsive part of the pseudopotential operator.

³⁸G. B. Bachelet, D. R. Hamann, and M. Schlüter, *Phys. Rev. B* **24**, 4745 (1981).

³⁹O. K. Andersen, O. Jepsen, and D. Glötzel, in *Highlights of Condensed Matter Theory*, edited by F. Bassani, F. Fumi, and

- M. P. Tosi (North-Holland, Amsterdam, 1985).
- ⁴⁰H. L. Skriver, in *The LMTO Method*, Vol. 41 of *Springer Series in Solid State Sciences*, edited by P. Fulde, M. Cardona, and H. Queisser (Springer, Berlin, 1981).
- ⁴¹S. S. Jaswal, *Phys. Rev. B* **34**, 8937 (1986); S. S. Jaswal, D. J. Sellmyer, M. Engelhardt, Z. Zhao, A. J. Arko, and K. Xie, *ibid.* **35**, 996 (1987).
- ⁴²S. K. Bose, S. S. Jaswal, O. K. Andersen, and J. Hafner, *Phys. Rev. B* **37**, 9955 (1988).
- ⁴³P. Steiner, H. Höchst, and S. Hufner, in *Photoemission in Solids II*, Vol. 27 of *Topics in Applied Physics*, edited by M. Cardona and L. Ley (Springer, Berlin, 1978), p. 349.
- ⁴⁴U. Mizutani and P. Oelhafen (private communication).
- ⁴⁵R. Car and M. Parrinello, *Phys. Rev. Lett.* **55**, 2471 (1985).
- ⁴⁶R. Car and M. Parrinello, *Phys. Rev. Lett.* **60**, 204 (1988).